Date of publication xxxx 00, 0000, date of current version xxxx 00, 0000.

Digital Object Identifier 10.1109/ACCESS.2017.Doi Number

Optimal Design of Elliptical Beam Cassegrain Antenna

XINGLONG LIU[1], BIAO DU[1], JIANZHAI ZHOU[1], and LEI XIE[1,2]

[1]The 54th Research Institute, China Electronics Technology Group Corporation, Shijiazhuang, 050081, China

[2] National Laboratory of Science and Technology on Antennas and Microwaves, Xidian University, Xi'an 710071, China

Corresponding author: Xinglong Liu (e-mail: xinglongxidian@163.com).

This work was supported by the National Natural Science Foundation of China under Grant BS61701456.

ABSTRACT An optimal design method of elliptical beam Cassegrain antenna based on differential evolution with global and local neighborhoods algorithm is proposed to achieve high efficiency, low sidelobe, and low profile at Ku/Ka dual band. A rapid shaping method of elliptical beam antenna is given by applying the algorithm of steepest descent. Constraining of the first sidelobe level, antenna efficiency is optimized with only 17 variables, where aperture field distribution functions in the major and minor axis planes are parameterized by Non-uniform rational B-spline curves, and the transition function is expressed with a sinusoidal function. A prototype of optimized antenna with an aperture of 630mm×1150mm is fabricated and measured. The measured results show that the total efficiency is greater than 54.5%, and the first sidelobe levels are lower than -14.2dB across the Ku/Ka dual-band, which agree well with simulated ones. It is verified that the optimal design method is very effective.

INDEX TERMS Reflector antenna, elliptical beam, low profile, dual-band, optimization algorithm

I. INTRODUCTION

With the rapid development of satellite communication technology, the demand for satellite mobile communication systems is increasing rapidly. As an essential component, the antenna for satellite communication on the move is required to be not only low profile, but also high gain, low side-lobe level, low cross-polarization, and even multi-band compatibility [1]-[3]. There are four main types of antenna with low profile for satellite communications on the move, a planar waveguide array antenna [4], phased array antenna [5], [6], Luneburg lens antenna [7] and elliptical beam reflector antenna [8]. The planar waveguide array antenna has a lower profile and high efficiency, but it is difficult to achieve high gain (for example, greater than 38dB in Ku band) and dual band operation (Ku/Ka dual-band), because of the loss increase of its feeding network and the bandwidth limit of the element and array. The phased array antenna has the lowest profile, fast and high precision beam tracking ability, but its beam scanning angle is limited, the gain will decrease and the sidelobe level will increase with beam scanning, in addition, its cost is high for the high gain requirements and it is also difficult to realize dual band operation. Hemispherical Luneburg lens antenna has a better beam scanning performance and can operate in dual-band, but its structure is relatively complex, weight is heavy, and profile is high for the high gain requirements. The elliptical beam reflector antenna has been widely used in satellite communication on the move, because of its good performance, simple structure and low profile. Hence, the elliptical beam reflector antenna is one of the ideal candidates of the medium and high gain antenna with good performances and low profile, especially with capability of dual-band operation.

Basically, there are two kinds of elliptical aperture shaping reflector antenna: elliptical beam ring-focus antenna and elliptical beam Cassegrain antenna. Both of them consist of axially-symmetric feed, non-rotationally symmetric main-reflector, and sub-reflector, having low profile, high efficiency and low cross-polarization. Due to the special geometry of ring-focus antenna, it is difficult to effectively control the elliptical aperture field distribution, hence its elliptical axis ratio is usually less than 1.5:1 [9],[10]. When its elliptical axis ratio increases to 2:1, the radiation patterns are distorted and first sidelobe levels (FSLLs) rise to -10dB [11]. The elliptical beam Cassegrain antenna is easy to achieve large axial ratio [12]. However, its FSLLs are also only about -10dB [13] or is only 1.5dB margin simulated by GRASP [8] (without considering the blockage caused by the actual feed), which cannot meet the engineering design requirements of FSLLs

This article has been accepted for publication in a future issue of this journal, but has not been fully edited. Content may change prior to final publication. Citation information: DOI 10.1109/ACCESS.2021.3109000, IEEE Access

below -14dB. Moreover, the classical aperture distributions which are used for shaping circular aperture reflector antenna, such as generalized Taylor displacement distribution, exponential distribution, and Hansen distribution, are not suitable for the elliptical aperture antenna shaping design. In [14] and [15], parameter aperture distribution, polynomial aperture distribution, and transition function based on the analysis method are chosen for elliptical beam antenna shaping design. However, the antenna cannot achieve the optimal electrical performance, especially for small aperture antenna.

Genetic algorithm, particle swarm optimization, ant colony optimization, and differential evolution are all bionic intelligence optimization algorithms, which can be used to find the global optimal solution. They have been used in various high-gain and microstrip antenna designs [16]-[19]. Besides, machine learning-based optimization algorithms such as multistage collaborative machine learning and neural networks have also been used in the design of microstrip antennas and filters [20]-[22], but require a large amount of data and time for training. Among these algorithms, differential evolutionary algorithms are known for their few variables, simplicity and efficiency in solving global optimization problems over continuous-spaces, and differential evolution with global and local neighborhoods (DEGL) algorithm introduces global and neighborhood optimal solutions into the mutation factor, which is easier to balance the exploration and exploitation abilities in optimization [23], and has been validated well in the optimized design of some high-gain reflector antennas.

This paper proposes an optimal design method of elliptic beam Cassegrain antenna based on DEGL algorithm. Firstly, the steepest descent method is introduced to shape the main- and sub-reflector curves in major and minor axis planes, which saves a lot of computing time so that the optimal design of the elliptical beam antenna becomes possible. Then, Non-uniform rational B-spline (NURBS) curve and sinusoidal function are adopted to represent the aperture field distributions with only 17 parameters. The optimal design method and procedure of elliptical beam Cassegrain antenna based on DEGL algorithm are presented. Finally, a Ku/Ka dual-band 630mm×1150mm elliptical beam antenna prototype is designed, fabricated, and measured. The measured results show that the total efficiency (including the losses of feeding network and waveguide) is greater than 54.5%, the FSLLs in azimuth plane and elevation plane are less than -14.5 dB and -14.2dB at Ku (12.25GHz-12.75GHz, 14GHz-14.5GHz) and Ka (19.6GHz-21.2GHz, 29.4GHz-31GHz) bands, respectively. The measured radiation patterns are in good agreement with the simulated ones, which verifies the correctness of the optimization design method.

Key contributions of this paper are as follows.

1) A steepest descent algorithm is proposed for the rapid shaping design of the elliptical beam antenna.
2) An optimal design method of elliptical beam Cassegrain antenna based on DEGL algorithm is presented, and a Ku/Ka dual-band elliptical beam Cassegrain antenna prototype is manufactured and excellent performance is achieved.

II. RAPID SHAPING DESIGN OF ELLIPTICAL BEAM ANTENNA

Fast shaping design is the basis of the optimal design of the elliptical beam Cassegrain antenna. The design method and procedure are given, and the steepest descent algorithm is introduced to calculate the sub-reflector curve in the major axis plane rapidly, which makes it possible to optimize the elliptical aperture reflector antenna.

A. SHAPING OF MAIN- AND SUB-REFLECTOR CURVES IN MAJOR AND MINOR AXIS PLANES

As shown in Fig. 1, the minor axis plane of the elliptical beam Cassegrain antenna is *XOZ* plane (i.e. $\varphi = 0°$ plane, the elevation plane), and the major axis plane is *YOZ* plane (i.e. $\varphi = 90°$ plane, the azimuth plane). $\boldsymbol{r}$, $\boldsymbol{m}$, and $\boldsymbol{s}$ are the vectors from the coordinate origin *O* (phase center of feed) to any point *S* on the sub-reflector, *O* to any point *M* on the main-reflector and the point *S* to *M*, respectively; θ_v is the angle between $\boldsymbol{s}$ with the -Z-axis; *P* is the intersection point between the curve of the sub-reflector and the *Z* axis (i.e. the vertex of the sub-reflector).

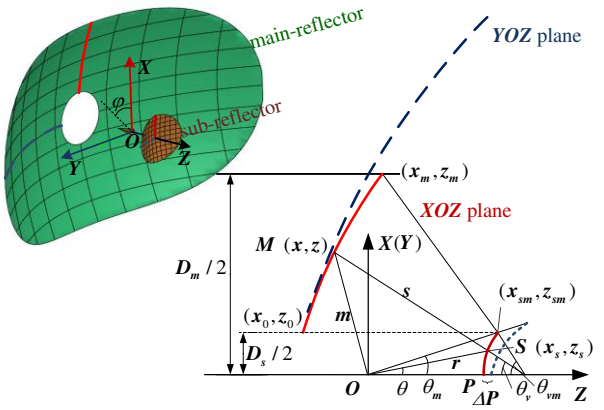

FIGURE 1. 3D view of the elliptical beam antenna and geometry of the shaping curves of the main- and sub-reflectors.

Firstly, the initial parameters in the minor axis plane are determined by the profile, gain, and geometry of antenna: the diameter of the main- and sub-reflector $D_{m0°}$, $D_{s0°}$, the half illumination angle of feed θ_m and the ratio of the focal length to the diameter $\tau_{0°}$. When the radiation pattern of feed $f(\theta)$ and the field distribution function of the main-reflector $F_{0°}(x)$ are selected, the partial differential equations for *x* and *r* can be obtained from the reflection law (Snell's law), the law of conservation of energy, equal optical path length condition [24]:

This article has been accepted for publication in a future issue of this journal, but has not been fully edited. Content may change prior to final publication. Citation information: DOI 10.1109/ACCESS.2021.3109000, IEEE Access

$$\begin{cases} \dfrac{dx}{d\theta} = A\dfrac{f^2(\theta)\sin\theta}{F^2(x)x} & x\big|_{\theta=\theta_m} = x_m \\ \dfrac{dr}{d\theta} = r\dfrac{x+(Ck-2r)tg\dfrac{\theta}{2}}{Ck-xtg\dfrac{\theta}{2}} & r\big|_{\theta=\theta_m} = r_m \end{cases} \tag{1}$$

where, Ck is the optical path length (constant). r and x will be solved by (1), thus obtaining the sub-reflector curve in the minor axis plane $r_{0^\circ}(\theta)$. With the same equal optical path length, θ_{vm} in the major axis plane can be obtained:

$$\theta_{vm90^\circ} = 2arc\cot\left(\frac{2Ck - D_{s90^\circ}tg\left(\theta_m/2\right)}{D_{m90^\circ} - D_{s90^\circ}}\right) \tag{2}$$

Similarly, the sub-reflector curve in the major axis plane $r_{90^\circ}(\theta)$ can be calculated by substituting D_{m90°, D_{s90°, θ_m, θ_{vm90°, $F_{90^\circ}(y)$, and $f(\theta)$ into (1), and replacing y for x in (1). In order to form an effective sub-reflector surface, the vertices of the sub-reflector in the major and minor axis planes must coincide ($|\Delta P| = |r_{90^\circ}(0) - r_{0^\circ}(0)| \le \varepsilon$). The value of D_{s90° determines the size of ΔP, and how to quickly determine D_{s90° is the key issue to the rapid shaping of elliptical beam antennas.

In this paper, an automatic rapid iteration loop is established using the steepest descent algorithm [25]. After k times' iteration, the diameter of the sub-reflector is calculated by

$$D_{s90^\circ}{}^{(k+1)} = D_{s90^\circ}{}^{(k)} - \frac{D_{s90^\circ}{}^{(k)} - D_{s90^\circ}{}^{(k-1)}}{\Delta P^{(k)} - \Delta P^{(k-1)}}\Delta P^{(k)} \tag{3}$$

Then, D_{s90° can be determined after a few number of iterations, until $|\Delta P| \le \varepsilon$, and then the sub-reflector surface curve $r_{90^\circ}(\theta)$ in the major axis plane is calculated.

Equation (3) introduces the gradient information into the iterative stepping, which can reduce the number of iterations to 3~4, and ΔP can achieve an accuracy of less than 1/1000 mm. Compared with the conventional algorithm that the number of iterations is 30~40, (3) can improve the calculation efficiency by about 10 times.

B. DETERMINING THE TRANSITION FUNCTION TO DESIGN THE SUB-REFLECTOR

The transition function is used to smoothly interpolate the sub-reflector surface curves between the minor and major axis planes to obtain a three-dimensional surface for the sub-reflector:

$$r(\theta,\varphi) = r_{0^\circ}(\theta) + (r_{90^\circ}(\theta) - r_{0^\circ}(\theta))T(\varphi) \tag{4}$$

where the transition function is described by a sine function:

$$T(\varphi) = \left(\sin\varphi\right)^{2q}, \quad q \in (0.8, 1.3) \tag{5}$$

The transition function has only one parameter of q. Changing the parameter q, the energy distribution in the φ direction can be controlled, and also the main-reflector profile can be controlled to approach a rectangle aperture (the maximum aperture), so as to maximize the antenna gain within the limited space. The transition function with different parameters and the corresponding aperture profile of the main-reflector are shown in Fig. 2. The optimal parameter q can be obtained by the optimization design in Section IV to achieve the balance between the energy distribution and the maximum aperture of the main-reflector.

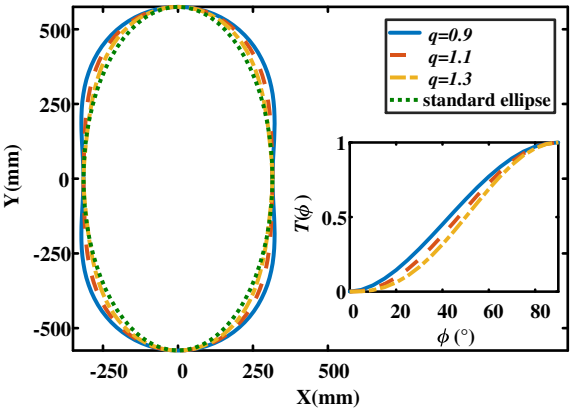

FIGURE 2. Transition functions with different values of *q* and corresponding contour of the main-reflector.

C. CALCULATION OF MAIN-REFLECTOR SURFACE OF THE ANTENNA

After determining the sub-reflector, the unit vector $\boldsymbol{e}_r$ of the vector $\boldsymbol{r}$, and the unit normal vector $\boldsymbol{e}_n$ of the sub-reflector are obtained. Based on Snell's law, the unit vector $\boldsymbol{e}_s$ of $\boldsymbol{s}$ can be obtained:

$$\boldsymbol{e}_s = \boldsymbol{e}_r - 2(\boldsymbol{e}_n \cdot \boldsymbol{e}_r)\boldsymbol{e}_n \tag{6}$$

Based on the equal optical path length condition, the main-reflector vector can be described as

$$\boldsymbol{m} = \boldsymbol{r} + \frac{Ck - r + r\boldsymbol{e}_r \cdot \boldsymbol{z}}{1 - \boldsymbol{e}_s \cdot \boldsymbol{z}} \tag{7}$$

Therefore, the main-reflector coordinates are obtained.

D. SHAPING DESIGN PROCEDURE

The design procedure of the elliptical beam Cassegrain antenna is described as the following 3 steps: Firstly, the main- and sub-reflector curves in the minor axis plane are calculated by the aperture distributions, the feed pattern, and geometric parameters. With the equal optical path length, these curves in the major axis plane are shaped by the method of steepest descent, and the diameter of the sub-reflector is iterated a few times until the vertices of sub-reflector curves in two planes are almost coincident. Secondly, transition function $T(\varphi)$ is selected to obtain the whole sub-reflector. Finally, the coordinates of the main-reflector are obtained based on Snell's law and the equal optical path length condition. The flow chart of the whole shaping design procedure of the elliptical beam Cassegrain antenna is shown in Fig. 3.

This article has been accepted for publication in a future issue of this journal, but has not been fully edited. Content may change prior to final publication. Citation information: DOI 10.1109/ACCESS.2021.3109000, IEEE Access

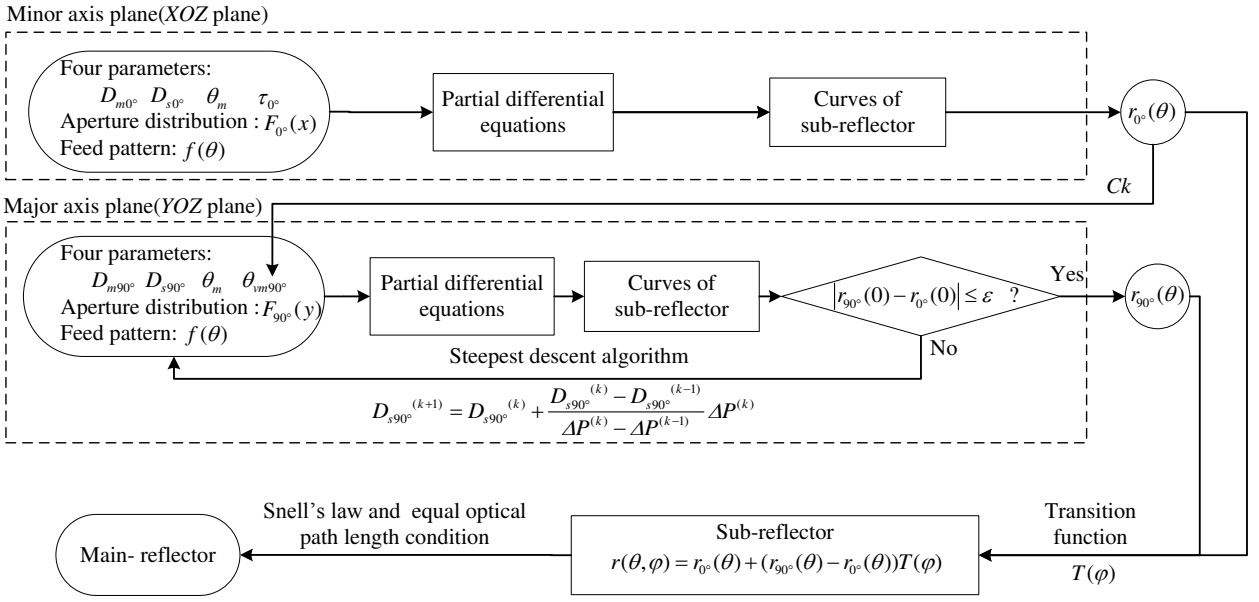

FIGURE 3. **Flow chart of shaping design of elliptical beam antenna.**

III. PARAMETERIZATION OF APERTURE DISTRIBUTION

Except the transition function expressed by sinusoidal function, the aperture field distributions in the major and minor axis plane plays an important role in the whole elliptical aperture energy distribution. In order to optimize the antenna performance, it is necessary to parameterize and optimize the field distribution functions.

NURBS has been widely used in CAD/CAM and computer graphics, due to its ability to accurately represent free-form curves and surfaces, with few control parameters, high flexibility, and local modifiability. It is also suitable for the parametric expression of the aperture field distribution function, such as *k*-th order NURBS curve [26] :

$$F(u) = \frac{\sum_{i=0}^{n} \omega_i d_i N_{i,k}(u)}{\sum_{i=0}^{n} \omega_i N_{i,k}(u)} \tag{8}$$

where, ω_i $(i=0,1,\ldots n)$ is the weighting factor, which is associated with the Z coordinates of control points d_i $(i=0,1,\ldots n)$, the first and last weighting factors $\omega_0, \omega_n > 0$, the remaining $\omega_i \ge 0$, and the constituent weight vectors W=[$\omega_0, \omega_1, \cdots \omega_n$]. $N_{i,k}(u)$ is the *k*-th order B-spline basis function, which can be obtained from the node vector $U = [u_0, u_1, \cdots u_i, \cdots u_{n+k+1}]$ according to the Debord-Cox recursion formula.

Based on the nodes vector U=[0 0 0 0 0.2 0.4 0.6 0.8 1 1 1 1], the coordinates of eight control points and the 3-order NURBS curve aperture distribution with different weight vectors are shown in Fig. 4. With the increase of the weight, NURBS curve approaches the control point. Therefore, the weight vector W=[1 1.4 1 1 1 1 1.4 1] is selected to express the aperture distribution curve.

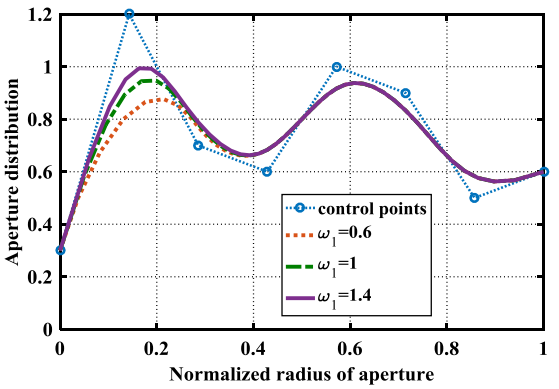

FIGURE 4. **NURBS curve of aperture distribution with different weights ω_1 (*W*1= [1 0.6 1 1 1 1 1.4 1], *W*2=[1 1 1 1 1 1 1.4 1] and *W*3=[1 1.4 1 1 1 1 1.4 1])**

Aperture field distribution functions in the major and minor axis planes are expressed by NURBS curves with 8 control points, respectively. Those coordinates and the transition function parameters *q* constitute the optimization vector of the antenna with only 17 variables ($X = [d_0, \cdots, d_i, \cdots, d_7, d'_0, \cdots, d'_i, \cdots, d'_7, q]$), which is much fewer compared to the orthogonal global expansion method [27].

IV. DEGL OPTIMIZATION DESIGN METHOD FOR ELLIPTICAL BEAM CASSEGRAIN ANTENNA

A. DEGL ALGORITHM

Compared with the classical DE algorithm [28], the concept of global and local neighborhood optimal combination is introduced in the mutation strategy of DEGL algorithm, which can balance the exploration and exploitation abilities [23][29], and its mutation is described as:

$$L_{i,G} = X_{i,G} + \alpha \cdot (X_{n\_best_i,G} - X_{i,G}) + \beta \cdot (X_{p,G} - X_{q,G})$$
$$g_{i,G} = X_{i,G} + \alpha \cdot (X_{g\_best,G} - X_{i,G}) + \beta \cdot (X_{r_1,G} - X_{r_2,G}) \quad (9)$$
$$V_{i,G} = \omega \cdot g_{i,G} + (1-\omega) \cdot L_{i,G}$$

where, $L_{i,G}$ and $g_{i,G}$ are local and global vector of G-th generation, respectively, $X_{n\_best,G}$ is the optimal individual in the $X_{i,G}$ neighborhood, $X_{g\_best,G}$ is the optimal individual of the entire population of generation G, both α and β are scaling factors. The weight factor ω can be represented by a linear function:

$$\omega = \omega_{\min} + (\omega_{\max} - \omega_{\min}) \cdot (G/G_{\max}) \quad (10)$$

where, ω will increase linearly from the minimum weight factor $\omega_{\min}$ to the maximum weight factor $\omega_{\max}$ as the evolutionary generation number G increases, ranging from 0 to 1. During the initial stages, ω is small, the neighborhood optimum plays a large role, which can accelerate the exploration. Then, ω becomes larger with the increase of G, as well as exploitation is improved，that can speed up the global convergence speed.

Compared with the existing evolutionary algorithm and particle swarm optimization, DEGL algorithm can greatly avoid falling into local optimum and premature problems, and has strong global optimization ability and fast convergence speed, which is suitable for the antenna optimization design [19].

B. OPTIMAL DESIGN OF ELLIPTICAL BEAM CASSEGRAIN ANTENNA

The optimal design of the elliptical beam Cassegrain antenna is aimed at maximizing the aperture efficiency, while constraining the FSLLs below $FSLL0_{\max}$ and $FSLL90_{\max}$ in the elevation plane and azimuth plane, respectively. The problem can be expressed as a minimization of the following function:

$$f(X) = 1 - \min_{1 \le n \le N} \{\eta_n\} \quad (11)$$

where, η_n is the efficiency of the antenna at the n-th frequency , and N is the number of frequencies. And the constraints are as follows:

$$g_1(X) = \max_{1 \le n \le N} \{FSLL0_n\} - FSLL0_{\max} \le 0 \quad (12)$$
$$g_2(X) = \max_{1 \le n \le N} \{FSLL90_n\} - FSLL90_{\max} \le 0 \quad (13)$$

where, $FSLL0_n$ and $FSLL90_n$ are the FSLLs at the n-th frequency in the elevation plane and the azimuth plane, respectively.

The above problem is transformed into an unconstrained optimization problem by the exact penalty function method. The fitness function is described as:

$$Fit(X) = f(X) + K \times \sum_{i=1}^{2} \max(g_i, 0) \quad (14)$$

Among them, K is the largest number of processing constraints. When the FSLL does not meet the object, the fitness is set to a large value, otherwise $Fit(X) \in (0,1)$, and the smallest $Fit(X)$ is corresponding to the best individual.

In summary, the general flow chart of the elliptical beam Cassegrain antenna optimization design based on DEGL algorithm is shown in Fig. 5. Set the scaling factor α =0.4, β =0.2, the minimum weight factor $\omega_{\min}$ =0.15, the maximum weight factor $\omega_{\max}$ =0.85, cross factor CR=0.3, population size NP=50 and maximum number of generations $G_{\max}$ =200. When the optimized algorithm is started, it will automatically model, simulate by physical optics and physical diffraction, analyze data, and iterate until the maximum number of generations is reached and the optimal individual is output.

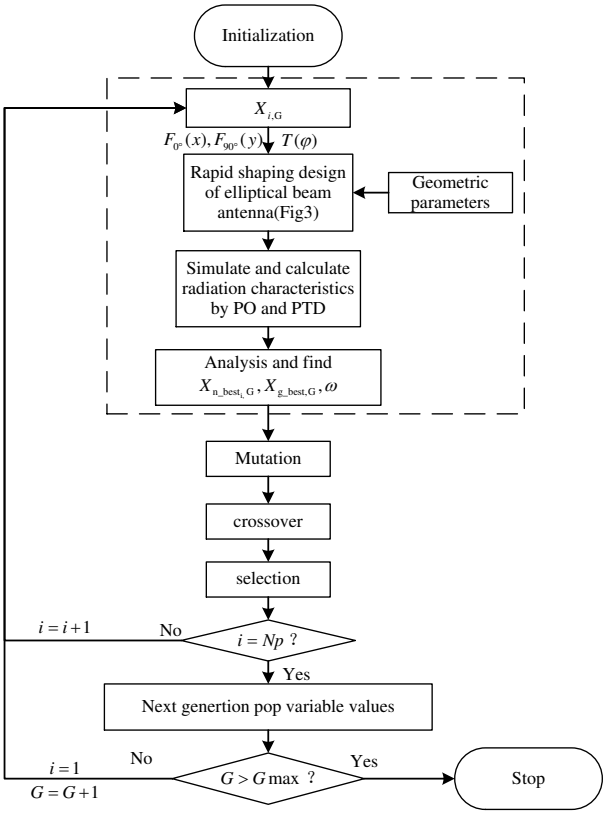

FIGURE 5. General flow chart of antenna optimization design based on DEGL algorithm

V. DESIGN EXAMPLE AND TEST VERIFICATION

The initial parameters are determined by the antenna requirement, as shown in Table 1. The diameter of the main- and sub-reflectors in the minor axis plane D_{m0° = 630 mm and D_{s0° = 150 mm, the half illumination angle of the feed θ_m = 36°, the illumination level of the feed is -10dB, the ratio of the focal length to the diameter τ = 0.65, and the diameter of the main- and sub-reflector in the major axis plane D_{m90° =1150 mm and D_{s90° =150 mm. The maximum FSLLs are constrained by $FSLL0_{\max}$ =-15 dB and $FSLL90_{\max}$ =-16 dB.

TABLE 1
SPECIFICATIONS OF ELLIPTICAL BEAM ANTENNA

Parameters	Specifications
1) Size of main-reflector	⩽ 630mm × 1150mm
2) Frequency(GHz)	Ku: 12.25-12.75;14-14.5 Ka: 19.6-21.2;29.6~31.0

This article has been accepted for publication in a future issue of this journal, but has not been fully edited. Content may change prior to final publication. Citation information: DOI 10.1109/ACCESS.2021.3109000, IEEE Access

Parameters	Specifications
3) FSLL(dB)	⩽-14
4) Aperture efficiency(%)	⩾60

In the optimization process, the analysis model of the antenna is established by GRASP software (PO/PTD) [16], [30]-[31]. After optimization, the transition function parameter q=0.96, the aperture distributions in the major and minor axis planes are shown in Fig. 6(a), and the two-dimensional elliptical aperture energy distribution of the shaped 630mm × 1150mm antenna is shown in Fig. 6(b).

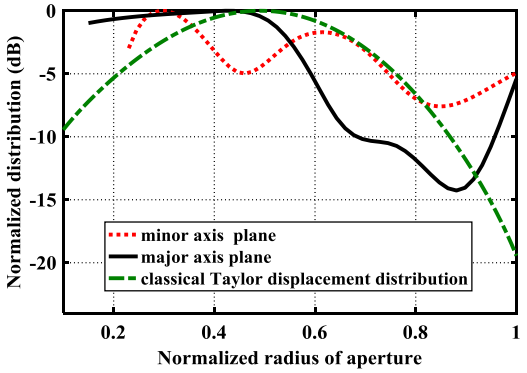

(a)

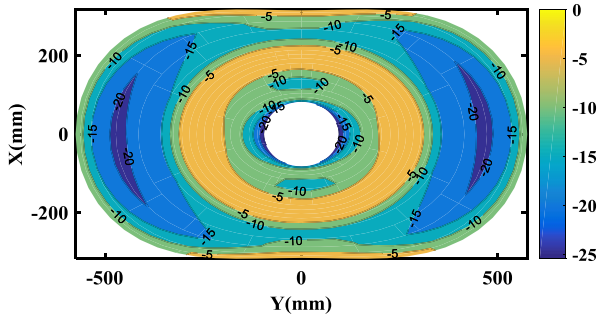

(b)

FIGURE 6. (a) Optimized aperture distribution curves in major- and minor- axis plane and (b) 2D elliptical aperture distribution.

It can be seen from Fig.6 that the optimized aperture field distribution is quite different from the classical Taylor displacement distribution. In the major axis plane, the aperture energy drops rapidly about 10~15dB in the middle of the radius, then rises by 8dB at the edge of the aperture, and there are two small oscillatory falls in the minor axis plane. The analysis shows that the rapid decrease of energy in the middle of the aperture in the major axis plane is beneficial to suppressing the sidelobe level of the antenna, while the increase of energy at the edge of the aperture is beneficial to improving the gain of the antenna. It can also be seen in Fig. 6(b) that the energy distributions in the major and minor planes are basically the same as the ones in Fig. 6(a), and the energy distribution between the major and minor planes is controlled by the transition function, which demonstrates that the optimal design method proposed in this paper can effectively control the elliptical aperture energy distribution.

The feed is designed using three ring loading grooves to obtain small aperture and axially-symmetric patterns across Ku/Ka dual-band, as shown in Fig. 7 [32].

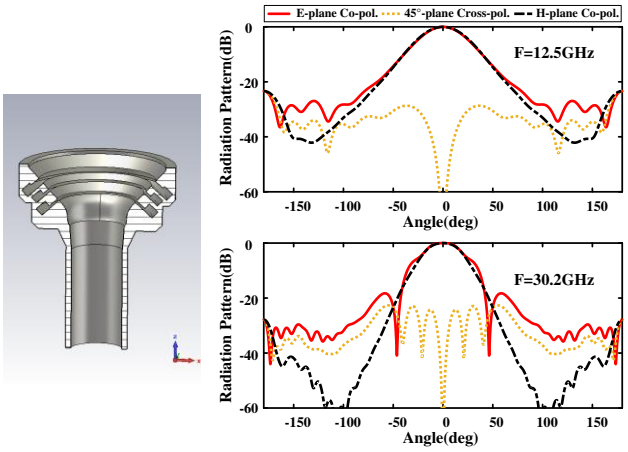

(a) (b)

FIGURE 7. (a) Model and (b) radiation patterns of Ku/Ka feed at 12.5GHz and 30.2GHz

CST model and photograph of the antenna prototype are given in Fig. 8. The equivalent diameter of the main-reflector of the antenna is 890 mm, which is increased by 9.3% compared with the equivalent diameter 851mm of the standard elliptical beam antenna. The calculated aperture efficiency of the antenna is above 64.6% in Ku band and 68.9% in Ka band, respectively. The FSLLs are below -15.1dB and -16.1dB in the elevation plane and azimuth plane, respectively.

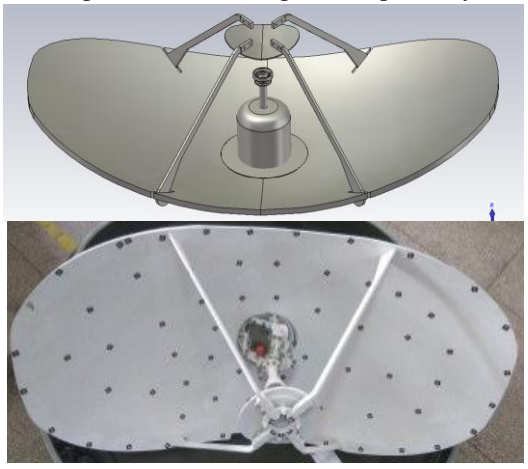

FIGURE 8. CST model and prototype of antenna

Fig. 9 shows the simulated and measured gain, efficiency, and FSLL at Ku/Ka dual-band. The measured total efficiencies are greater than 54.5%, basically the same as the simulated ones when considering the loss of feeding network (0.3-0.6dB). The simulated and measured FSLLs in elevation and azimuth plane are below -14.2dB and -14.5dB, respectively, which has met the requirements. If the FSLL needs to be further reduced, we can apply the optimized design method proposed in this paper, change the constraints

This article has been accepted for publication in a future issue of this journal, but has not been fully edited. Content may change prior to final publication. Citation information: DOI 10.1109/ACCESS.2021.3109000, IEEE Access

of the FSLL, and optimize the aperture distribution. In this way, we can achieve lower FSLL, but at the expense of antenna gain. Moreover, Fig. 10 shows the simulated and measured radiation patterns of the antenna at 12.5 GHz, 14.25 GHz, 20.4 GHz and 30.2 GHz in the azimuth and elevation planes. It can be seen that the measured patterns are in good agreement with the simulated ones, especially in the angular range of $\pm 5°$. The measured elliptical beam pattern axis ratio is about 1.8:1, and the cross polarization on boresight is below -35dB at Ku band, and the axis-ratio of circular polarization is lower than 1.5dB at Ka band. Fig.11 shows the simulated and measured $|S_{11}|$ of antenna at Ku and Ka bands. It can be observed that they are basically consistent, and $|S_{11}|$ at Ku and Ka bands are lower than -14.5dB and -17.0dB, respectively. The above results demonstrate the effectiveness and correctness of the design method.

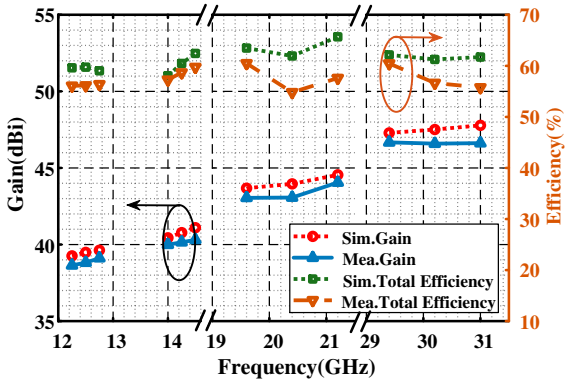

(a)

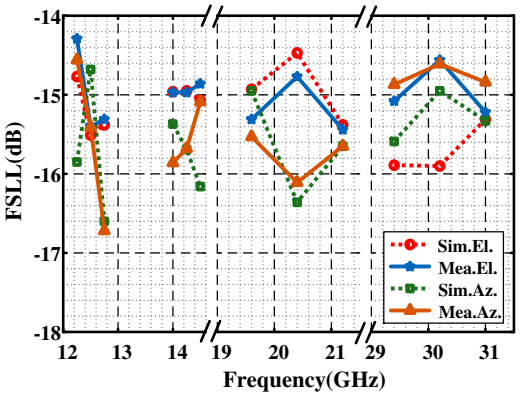

(b)

FIGURE 9. (a)Simulated and measured gain, efficiency, and (b) FSLL in azimuth plane and elevation plane at Ku/Ka band

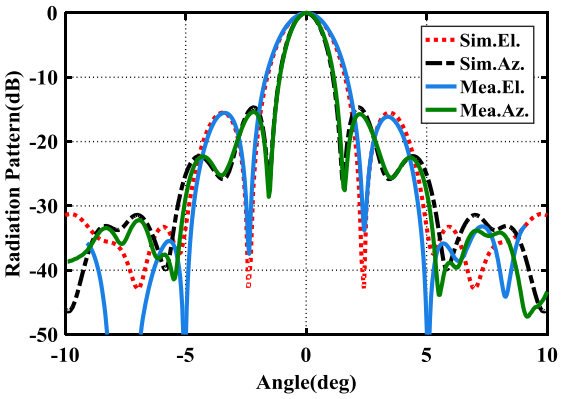

(a)

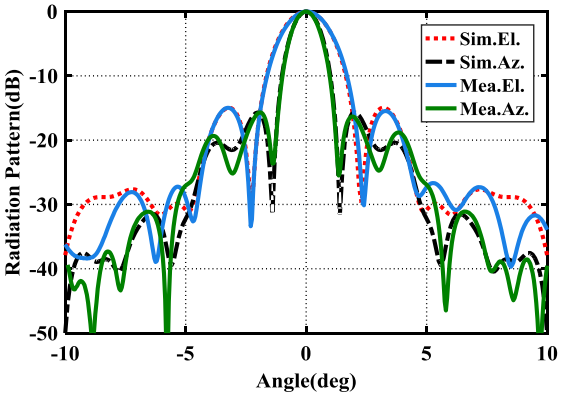

(b)

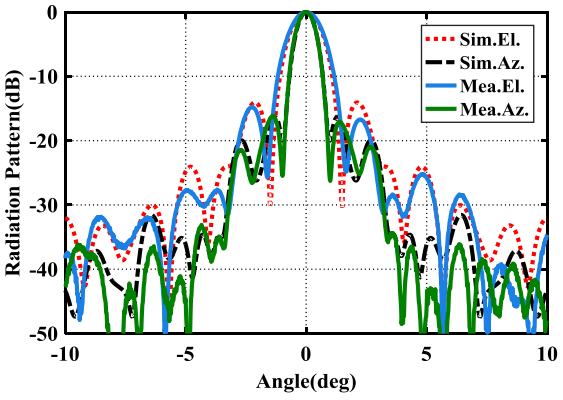

(c)

This article has been accepted for publication in a future issue of this journal, but has not been fully edited. Content may change prior to final publication. Citation information: DOI 10.1109/ACCESS.2021.3109000, IEEE Access

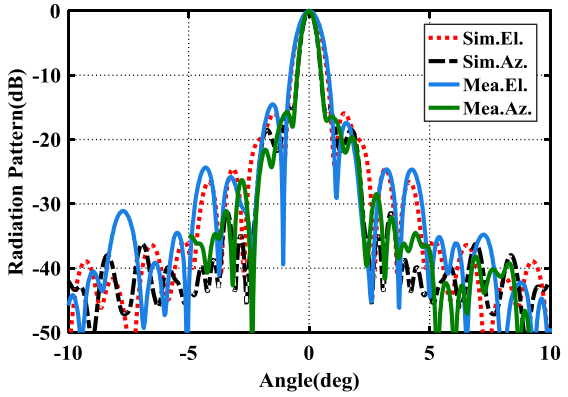

(d)

FIGURE 10. Simulated and measured radiation patterns (a) 12.5GHz, (b) 14.25GHz, (c) 20.4GHz, and (d) 30.2GHz.

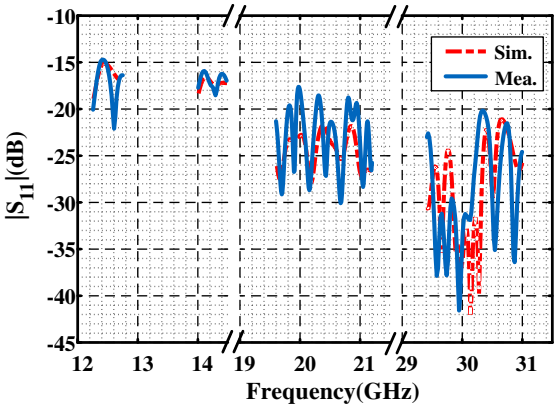

FIGURE 11. (a)Simulated and measured gain, efficiency, and (b) FSLL in azimuth plane and elevation plane at Ku/Ka band

In addition, the performance of previously reported elliptical-beam antennas and this prototype are compared in Table 2. The reported antennas [4]-[9] operate at only one band or at one frequency, and measured FSLLs are worse than -14dB, and the measured total efficiency is not given. It is noticed that the prototype developed by the proposed method can cover the Ku/Ka dual-band with relatively low FSLLs below -14dB in both elevation and azimuth plane. Furthermore, the measured total efficiency of antenna including feed and network is more than 54.5%, and the aperture axis ratio is up to 1.83:1. Therefore, the antenna prototype shows better performances.

TABLE 2
PERFORMANCES OF ELLIPTICAL BEAM ANTENNA

Ref.	Frequency (GHz)	FSLL(dB) (Az., El.)	Gain (dBi)	Aperture efficiency(%)	Total Efficiency(%)	Ant. aperture (λ×λ)	Aperture axis ratio
[4]	12.5, 14.25	-14.0, -20.0	-	-	-	28.3× 18.8	1.51:1
[5]	-	-13.0, -11.0	-36.1	-	-	42.4 × 26.8	1.58:1
[6]	12.0	-10.3, -12.5	37.7	74.6	-	40 × 20	2:1
[7]	-	-23.0, -18.0(Sim.)	44.6(Sim.)	65.0(Sim.)	-	100 × 50	2:1
[8]	11.2-12.8, 14.0-14.4	-7.0,-15.0	30.5,32.7	-	-	-	-
[9]	12.25-12.75, 14.0-14.5	-13.5, -15.5(Sim.)	38.4, 39.8(Sim.)	62.0	-	44.9× 22.5	2:1
This work	12.25-12.75, 14.0-14.5, 19.6-21.2, 29.4-31.0	-14.2, -14.5	38.6,40.0, 43.0,46.0(Total)	64.6	54.5	47× 25.7	1.83:1

*The λ denotes the wavelength in free space at the lowest operating frequency of antenna.

VI. CONCLUSION

An optimal design method of elliptical beam Cassegrain antenna based on DEGL algorithm is proposed. A steepest descent algorithm is used for the rapid shaping design of the antenna. The NURBS curve and sinusoidal function are adopted to describe two aperture field functions and one transition function with only 17 parameters. The optimal aperture field distribution curves and the design of an elliptical beam Cassegrain antenna with the axis ratio 1.8:1 at Ku/Ka dual-band are achieved by optimizing the antenna efficiency and constraining the FSLL. The antenna prototype is fabricated and measured. The test results of antenna efficiency, FSLL and pattern are consistent with the simulation ones, which verify the correctness of the optimization design method in this paper. The antenna has been widely used in many engineering projects. This method can also be used for the optimization design of dual reflector antennas with arbitrary axis ratio elliptical beam.

REFERENCES

[1] K. Aoki, N. Miyahara, S. Makino, S. Urasaki, and T. Katagi, "Design method for offset shaped dual-reflector antenna with an elliptical aperture of low cross-polarization characteristics," *IEE Proc.-Microw. Antennas Propag.*, vol.146, no.1, pp. 60-64, Feb. 1999.

[2] E. Martinez-de-Rioja, J. A. Encinar, M. Barba, R. Florencio, R. R. Boix, and V. Losada, "Dual polarized reflectarray transmit antenna for operation in Ku- and Ka-bands with independent feeds," *IEEE Trans. Antennas Propag.*, vol. 65, no. 6, pp. 3241-3246, Jun. 2017.

[3] F. Greco, L. Boccia, E. Arnieri, and G. Amendola, "K/Ka-band cylindrical reflector antenna for compact satellite earth terminals," *IEEE Trans. Antennas Propag.*, vol. 67, no. 8, pp. 5662-5667, Aug. 2019.

[4] M. Ferrando-Rocher, J. I. Herranz-Herruzo, A. Valero-Nogueira, and B. Bernardo-Clemente, "Full-metal K-Ka dual-band shared-aperture array antenna fed by combined ridge-groove gap waveguide," *IEEE Antennas Wireless Propag. Lett.*, vol. 18, no. 7, pp. 1463-1467, Jul. 2019.

[5] G. Han, B. Du, W. Wu, and B. Yang, "A novel hybrid phased array antenna for satellite communication on-the-move in Ku-band," *IEEE Trans. Antennas Propag.*, vol. 63, no. 4, pp. 1375-1383, Apr. 2015.

[6] A. H. Aljuhani, T. Kanar, S. Zihir, and G. M. Rebeiz, "A 256-element Ku-band polarization agile satcom receive phased array with wide-angle scanning and high polarization purity," *IEEE Trans. Microw. Theory Techn.*, vol. 69, no. 5, pp. 2609-2628, May 2021.

[7] N. Nikolic and A. Hellicar, "Fractional luneburg lens antenna," *IEEE Antennas Propag. Mag.*, vol. 56, no. 5, pp. 116-130, Oct. 2014.

[8] X. L. Liu, B. Du, S. Y. Qin, "A low profile, high efficiency and large axis ratio elliptic beam antenna," *Chinese J. of Radio Science*, vol. 26, Sup., pp. 505-508, Oct. 2011.

[9] Z. Y. Lu, "A efficient ring-focus antenna for forming an elliptic beam," in *Proc. Int. Conf. Microw. and Millimeter Wave. Technol. (ICMMT)*, Chengdu, China, 2010, pp. 1880-1882.

[10] S. H. He, M. Q. JI, and L. Y. XIE, "An improved design method for ring-focus reflector antenna with elliptical beam," in *Proc. Int. Symp. Ant. Propag. (ISAP)*, Xi'an, China, 2019, pp.1-3.

[11] J. M. Wu, L. Xie, D. F. Zhou, L. Hou, and H. W. Chen, "Design of ring-focus elliptical beam reflector antenna," *Int. J. of Ant. Propag.*, vol. 2016, 7 pages, doi:10.1155/2016/9615064.

[12] K. W. Brown and A. Prata, "Elliptical beam closed-form dual-reflector antenna efficiently illuminated by a feed with an axially-symmetric radiation pattern," in *Proc. IEEE Antennas Propag. Society Int. Symp. (APSURSI)*, Newport Beach, CA, USA, Jun. 1995, pp. 877-880 vol. 2.

[13] Y. Inasawa, S. Kuroda, K. Kusakabe, I. Naito, Y. Konishi, S. Makino, and M. Tsuchiya, "Design method for a low-profile dual-shaped reflector antenna with an elliptical aperture by the suppression of undesired scattering," *IEICE Trans. Electron.,* vol. E91-C no. 4 pp. 615-624, Apr. 2008, doi:10.1093/ietele/e91-c.4.615.

[14] D. Duan and Y. Rahmat-Samii, "A generalized three-parameter aperture distribution for antenna applications," *IEEE Trans. Antennas Propag.*, vol. 40, no. 6, pp. 27-40, Jun. 1992.

[15] X. L. Liu, B. Du, S. Y. Qin, and J. Z. Zhou, "Study of Transition Function for Elliptical Beam Antenna with Large Axial Ratio," *J. of CAEIT*, vol. 7, no. 1, pp. 72-75, Feb. 2012, doi: 10.3969/j.issn.1673-5692.2012.01.014.

[16] S. C. Pavone, A. Mazzinghi, and M. Albani, "PO-based automatic design and optimization of a millimeter-wave sectoral beam shaped reflector," *IEEE Trans. Antennas Propag.*, vol. 68, no. 6, pp. 4229-4237, Jun. 2020.

[17] N. Jin and Y. Rahmat-Samii, "Parallel Particle Swarm Optimization and Finite-Difference Time-Domain (PSO/FDTD) Algorithm for Multiband and Wide-Band Patch Antenna Designs," *IEEE Trans. Antennas Propag.*, vol. 53, no. 11, pp. 3459-3468, Nov. 2005.

[18] C. M. Coleman, E. J. Rothwell, and J. E. Ross, "Investigation of simulated annealing, ant-colony optimization, and genetic algorithms for self-structuring antennas," *IEEE Trans. Antennas Propag.*, vol. 52, no. 4, pp. 1007-1014, Apr. 2004.

[19] T. L. Zhang, L. Chen, Z. H. Yan, and B. Li, "Design of dual offset shaped reflector antenna based on degl algorithm," *J. of Electromagnetic Waves & Appl.*, vol. 25, pp. 723-732, Apr. 2011, doi: info:doi/10.1163/156939311794827339.

[20] Q. Wu, H. Wang and W. Hong, "Multistage collaborative machine learning and its application to antenna modeling and optimization," *IEEE Trans. Antennas Propag.*, vol. 68, no. 5, pp. 3397-3409, May 2020.

[21] L. -Y. Xiao, W. Shao, F. -L. Jin, B. -Z. Wang, and Q. H. Liu, "Inverse artificial neural network for multi-objective antenna design," *IEEE Trans. Antennas Propag.*, Apr. 2011, doi: 10.1109/TAP.2021.3069543.

[22] M. Jamshidi, A. Lalbakhsh, B. Mohamadzade, H. Siahkamari, and S. M. H. Mousavi, "A novel neural-based approach for design of microstrip filters" *Int. J. Electron. Commun. (AEU)*, Jul. 2019, doi: 10.1016/j.aeue.2019.152847.

[23] U. K. Chakraborty, S. Das, and A. Konar, "Differential evolution with local neighborhood," in *Proc. IEEE Int. Conf. Evol. Comput. (CEC)*, Vancouver, BC, Canada, Jul. 2006, pp. 2042-2049.

[24] V. Galindo, "Design of dual-reflector antennas with arbitrary phase and amplitude distributions," *IEEE Trans. Antennas Propag.*, vol. 12, no. 4, pp. 403-408, Jul. 1964, doi: 10.1109/TAP.1964.1138236.

[25] Y. Ichioka, Y. Takubo, K. Matsuoka, and T Suzuki, "Iterative image restoration by a method of steepest descent", *Journal of Optics*, vol. 12, no. 1, pp. 12-35, 1981.

[26] L. Piegl, and W. Tiller, *The NURBS Book*. Berlin, Germany: Springer, 1997.

[27] Dah-Weih Duan, and Yahya Rahmat-Samii, "A generalized diffraction synthesis technique for high performance reflector antennas," *IEEE Trans. Antennas Propag*., vol. 43, no. 1, pp. 27-40, Jan. 1995.

[28] R. Storn, and K. V. Price, "Differential evolution-a simple and efficient heuristic for global optimization over continuous space," *J. Glob. Optim.*, vol. 11, no. 4, pp. 341-359, 1997, doi: 10.1023/A:1008202821328.

[29] S. Das, A. Abraham, U. K. Chakraborty, and A. Konar, "Differential evolution using a neighborhood-based mutation operator," *IEEE Trans. Evol. Comput*., vol. 13, no. 3, pp. 526-553, Jun. 2009.

[30] Z. Lei, "Radiation pattern analysis of reflector antennas using cad model-based physical optics method," *IEEE Access*, vol. 7, pp. 162598-162604, Nov. 2019.

[31] TICRA, Grasp10 Version 10.0, Denmark[Online]. Available: http://tica.com

[32] L. Xie, Y. C. Jiao, B. Du, Z. Y. Meng, and Y. Shi. "Optimal design of a Ku/Ka-band wide-flare-angle corrugated horn using the differential evolution algorithm," *Progress In Electromagnetics Research Letters*, vol. 59, pp. 27-33, Mar. 2016, doi: 10.2528/pierl16012508.